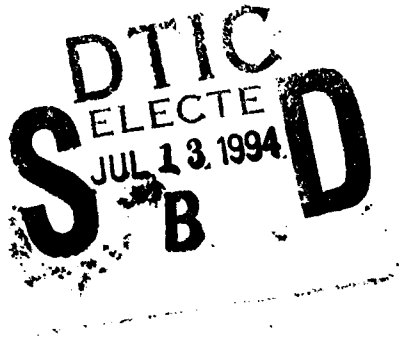

OFFICE OF NAVAL RESEARCH

GRANT: N00014-90-J-1230

R&T CODE 4133015

ROBERT J. NOWAK

Technical Report No. 59

Cyclic Voltammetric Analysis of Ferrocene Alkanethiol Monolayer Electrode Kinetics Based on Marcus Theory

by

L. Tender, M. T. Carter, and R. W. Murray

Prepared for Publication

in

Analytical Chemistry

University of North Carolina at Chapel Hill
Department of Chemistry
Chapel Hill, NC

July 1, 1994

REPORT DOCUMENTATION PAGE

Form Approved
OMB No. 0704-0188

1. AGENCY USE ONLY (Leave blank)	2. REPORT DATE	3. REPORT TYPE AND DATES COVERED
	July 1, 1994	Interim May 93 - Jun 94

4. TITLE AND SUBTITLE
Cyclic Voltammetric Analysis of Ferrocene Alkanethiol Monolayer Electrode Kinectics Based on Marcus Theory

5. FUNDING NUMBERS
N00014-90-J-1230

6. AUTHOR(S)
L. Tender, M. T. Carter, and R. W. Murray

7. PERFORMING ORGANIZATION NAME(S) AND ADDRESS(ES)
The University of North Carolina at Chapel Hill
Department of Chemistry
Chapel Hill, N.C. 27599-3290

8. PERFORMING ORGANIZATION REPORT NUMBER
Tech. Report 59

9. SPONSORING/MONITORING AGENCY NAME(S) AND ADDRESS(ES)
Office of Naval Research
Department of the Navy
Arlington, VA 22217

10. SPONSORING/MONITORING AGENCY REPORT NUMBER

11. SUPPLEMENTARY NOTES

12a. DISTRIBUTION AVAILABILITY STATEMENT
Approved for Public Release, Distribution Unlimited

12b. DISTRIBUTION CODE

13. ABSTRACT *(Maximum 200 words)*

Theory for electrode kinetics of surface-immobilized monolayers in cyclic voltammetry is developed based on the Marcus free energy-rate relation. Numerical calculations show that when the applied over-potential exceeds ca. 30% of the reorganizational energy of the electrode reaction, voltammetry predicted from Marcus theory differs from that based on classical Butler-Volmer kinetics with regard to waveshape, peak currents and their dependence on potential sweep rate, and variation of peak potential with potential sweep rate. Estimates of the standard rate constant, k^o, can be made from E_{PEAK} data without exact knowledge of reorganizational energies. Examples are given of evaluating k^o for monolayers of ferrocene alkanethiols chemisorbed on Au(111) electrodes, when the monolayers are highly ordered, and kinetically monodisperse, and when they are somewhat disordered, and kinetically disperse on bulk gold electrodes at room and 150K temperatures.

14. SUBJECT TERMS
Electrode kinetics, monolayers, cyclic voltammetry, Marcus equation

15. NUMBER OF PAGES

16. PRICE CODE

17. SECURITY CLASSIFICATION OF REPORT	18. SECURITY CLASSIFICATION OF THIS PAGE	19. SECURITY CLASSIFICATION OF ABSTRACT	20. LIMITATION OF ABSTRACT
UnClassified	UnClassified	UnClassified	Unlimited

June 20, 1994

CYCLIC VOLTAMMETRIC ANALYSIS OF FERROCENE ALKANETHIOL MONOLAYER ELECTRODE KINETICS BASED ON MARCUS THEORY

Leonard Tender[a], Michael T. Carter, and Royce W. Murray*

Kenan Laboratories of Chemistry

University of North Carolina, Chapel Hill, NC 27599-3290

ABSTRACT

Theory for electrode kinetics of surface-immobilized monolayers in cyclic voltammetry is developed based on the Marcus free energy-rate relation. Numerical calculations show that when the applied over-potential exceeds ca. 30% of the reorganizational energy of the electrode reaction, voltammetry predicted from Marcus theory differs from that based on classical Butler-Volmer kinetics with regard to waveshape, peak currents and their dependence on potential sweep rate, and variation of peak potential with potential sweep rate. Estimates of the standard rate constant, k^o, can be made from E_{PEAK} data without exact knowledge of reorganizational energies. Examples are given of evaluating k^o for monolayers of ferrocene alkanethiols chemisorbed on Au(111) electrodes, when the monolayers are highly ordered, and kinetically monodisperse, and when they are somewhat disordered, and kinetically disperse on bulk gold electrodes at room and 150K temperatures.

[a]Present address: Department of Chemistry, University of California, Berkeley, CA 94707

CYCLIC VOLTAMMETRIC ANALYSIS OF FERROCENE ALKANETHIOL MONOLAYER ELECTRODE KINETICS BASED ON MARCUS THEORY

Theory enabling measurement of heterogeneous electron transfer rates from cyclic voltammetric oxidation-reduction peak potential separations, ΔE_{PEAK} was presented some time ago by Nicholson and Shain[1] for diffusing and by Laviron[2] for diffusionless (i.e., surface bound) electrochemical systems. This methodology is appealing by its ease of application; standard electron transfer rate constants (k^o) result from analysis of the dependence of ΔE_{PEAK} values on potential sweep rate using numerically generated working curves[1] or explicit expressions[2]. These theoretical formulations are based on the Butler-Volmer[3] free energy-rate relation, which in the context of modern electron transfer theory due to Marcus[4], assumes that the applied potential (free energy, over-potential, $\eta = E - E^{\circ\prime}$) is much smaller than the electrode reaction's reorganizational energy barrier (λ).

This paper will describe the theoretical and experimental behavior of cyclic voltammetry of non-diffusing (immobilized) electrode reactants when η is not negligible in comparison to λ, i.e., in or approaching what is commonly referred to as the Marcus inverted region[4,5]. This contribution is made in the context of recent potential step experiments[6,7] with electroactive, self-assembled monolayers in which the ratio η/λ is not small. Co-chemisorption of a mixture of the alkanethiols $CH_3(CH_2)_{15}SH$ and $CpFeCpCO_2(CH_2)_{16}SH$ (Cp = cyclopentadienyl) on Au(111) produces a dilute layer of ferrocene sites that are separated, sometimes quite uniformly, from the Au surface by the alkane chains. This tunnelling barrier depresses the ordinarily fast $CpFeCp^{0/+}$ electron transfer rates to values sufficiently slow as to be readily measurable[6] even when large over-

potentials (η) are applied in potential step experiments. Since the Butler-Volmer relation[3] is inappropriate when η/λ is not small, the Marcus[4,5] equation, integrated over the continuum of electronic energies of the electrode[8], was employed for analysis of the observed[6] over-potential-rate results.

While the potential step experiment and its analysis for electron transfer rate constants of self-assembled monolayers are straightforward, cyclic voltammetric experiments are also straightforward and can be less tedious to carry out. Rate analysis of potential sweep data requires a solution of the combined potential sweep voltammetry-Marcus theory problem, which is the thrust of this paper. Our numerical (finite difference) calculations reveal that voltammetry under conditions of comparable over-potential and reorganizational energy has characteristics differing substantially from the familiar voltammetry of Butler-Volmer electrode kinetics[2]. The calculations are presented as working curves convenient for measurement of standard electron transfer rate constants k^o using ΔE_{PEAK} values. Good estimates of k^o can be obtained from ΔE_{PEAK} data without assumptions about values of reorganization energy (λ). The peak currents and shape of the voltammetric wave are very sensitive to λ, but reorganizational energy λ is reliably obtained from peak currents and shape only when the electroactive layer is kinetically monodisperse. The theoretical results are illustrated by application to three cases of experimental voltammetry of ferrocene alkanethiol monolayers.

EXPERIMENTAL

Chemicals. $CpFeCpCO_2(CH_2)_{16}SH$ and $CpFeCpCO_2(CH_2)_{18}SH$ were prepared by literature methods.[9] Alkanethiols (hexadecyl and octadecyl, Aldrich, > 97%), absolute ethanol

(AAPER Alcohol and Chemical Co.) and perchloric acid (Fisher, 11.1 N aq.) were used as received. Water was purified with a Barnstead Nanopure system.

Electrode Fabrication. The evaporated gold working electrode used for the data in Figures 6 and 7 consisted of 2000 Å of gold and a 150 Å titanium underlayer evaporated at room temperature at ca. $1x10^{-7}$ torr onto a silicon (100) substrate. An open bottom glass electrochemical cell was employed in which the working electrode served as the cell bottom and the electrode area (0.7 cm^2) was defined by a sealing rubber "o"-ring positioned between the electrode and the glass cell. Ag/(aq. 1M $AgClO_4$) reference electrode and Pt wire counter electrodes were employed in 1M $HClO_4$ electrolytic solution.

The bulk gold electrodes used in Figures 8 and 9 (1 mm radius) and Figures 10 and 11 (0.25 mm radius) were fabricated by attaching a Teflon® shrouded copper wire with silver solder (Kester) to ca. 1 cm long gold wires (Aldrich, 99.99 %). The two wires were encapsulated together in a cylinder of insulating epoxy (Shell Epon 828, m-phenylenediamine curing agent, cured overnight at 70° C), and sanded (Buehler 600 grit) to expose gold areas of 0.0314 and 0.0019 cm^2, respectively. For aqueous experiments, SCE reference and Pt flag counter electrodes were employed in a three compartment glass cell with the larger gold working electrode. The electrolyte was 1 M $HClO_4$. For low temperature experiments (see below), the smaller gold disk was used as the working electrode and the large gold disk was employed as a quasi-reference electrode.

Chemisorbed Ferrocene Monolayer Preparation. The evaporated gold electrode used in Figures 6 and 7 was after fabrication immediately immersed into 1 mM $CpFeCpCO_2(CH_2)_{18}SH$ and 1 mM $CH_3(CH_2)_{17}SH$ in ethanol to soak undisturbed at room

temperature for 3 days, followed by a rinse with ethanol and a further 10 days soak in 1 mM $CH_3(CH_2)_{17}SH$ in ethanol to exchange loosely bound ferrocene sites out of the film.

The 0.0314 cm^2 bulk gold electrode used in Figures 8 and 9 was polished with aqueous slurries of successively finer alumina powder (down to 0.05 μm, Buehler), sonicated for 5 min. in water, and rinsed with water followed by ethanol. Finally, to ensure removal of alumina from the gold surface, the electrode was polished with 0.25 μm diamond paste (Buehler), rinsed extensively with water and sonicated in ethanol. The electrode was etched in dilute aqua regia (3:1:6 $HCl:HNO_3:H_2O$) for 5 min,[10] rinsed with water, and ethanol and then immersed in an ethanol solution of 0.5 mM $CpFeCpCO_2(CH_2)_{16}SH$ and 0.5 mM $CH_3(CH_2)_{15}SH$ for 3 days. After rinsing with ethanol the electrode was soaked for an additional 7 days in 1 mM $CH_3(CH_2)_{15}SH$ in ethanol. For low temperature work, the electrode, polished and etched as above, was soaked for 6 days at room temperature in an ethanolic solution containing 0.25 mM $CpFeCpCO_2(CH_2)_{16}SH$ and 0.75 mM $CH_3(CH_2)_{15}SH$, then rinsed with ethanol and used without annealing in alkanethiol solution. The large Au disk, serving as quasi-reference, was abraded with fine grit sandpaper to remove surface thiol.

Low Temperature Voltammetry. Experiments at low temperature (150K) were performed in an electrolyte solution composed of 2:1 (v:v at RT) chloroethane (EtCl) and butyronitrile (PrCN) and 0.075 M Bu_4NPF_6 electrolyte. A Janis/Leybold closed cycle helium cryostat was employed in which the electrochemical cell is mounted directly on the cold head of the cryostat. The electrode configuration has been reported previously[11]. Electrochemical equipment was locally constructed and of conventional design.

RESULTS AND DISCUSSION

Electron Transfer Kinetic Theory. For a simple, reversible electron transfer reaction between a metal electrode and an attached redox species

$$Ox + e^- \underset{k_{Ox,\eta}}{\overset{k_{Red,\eta}}{\rightleftharpoons}} Red \qquad (1)$$

the dependency of $k_{Red,\eta}$ and $k_{Ox,\eta}$ (the forward and reverse η-dependent half reaction rate constants) on η as expressed by the Butler-Volmer relations is

$$k_{red,\eta} = k^o \exp(-\frac{\eta}{2k_BT}) \qquad (2)$$

$$k_{ox,\eta} = k^o \exp(\frac{\eta}{2k_BT}) \qquad (3)$$

where $\eta = E - E^{o\prime}$, k_B is the Boltzmann constant, T the temperature, k^o the standard rate constant, and the transfer coefficient[3], α, is assumed to equal to 0.5. The analogous Marcus relations[4,5]

$$k_{red,\eta} = k^o \exp(-\frac{\eta}{2k_BT} - \frac{\eta^2}{4\lambda k_BT}) \qquad (4)$$

$$k_{ox,\eta} = k^o \exp(\frac{\eta}{2k_BT} - \frac{\eta^2}{4\lambda k_BT}) \qquad (5)$$

reduce to the Butler-Volmer equations when $\eta/\lambda \ll 1$. The Marcus relations[4,5] predict that, as η approaches λ, the rate constants do not continue to increase exponentially with η (as they always do in the Butler-Volmer formulation) but maximize at $\eta = \pm \lambda$ and actually

decrease at larger η (classical Marcus "inverted" region). When electron transfers occur at a metal interface, however, it is necessary to account for the energy distribution of electrons about the Fermi level in the metal which, following Chidsey[6], leads to

$$k_{red,\eta} = \mu \rho k_B T \int_{-\infty}^{\infty} \frac{\exp\{-(x-\frac{\lambda+\eta}{k_B T})^2 \frac{k_B T}{4\lambda}\}}{1+\exp(x)} dx \qquad (6)$$

$$k_{ox,\eta} = \mu \rho k_B T \int_{-\infty}^{\infty} \frac{\exp\{-(x-\frac{\lambda-\eta}{k_B T})^2 \frac{k_B T}{4\lambda}\}}{1+\exp(x)} dx \qquad (7)$$

where χ is electron energy relative to the Fermi level, μ is the distance dependent electronic coupling between electrode and redox sites and ρ is the density of electronic states in the metal electrode. μ is anticipated to depend exponentially on distance, d, according to[7],

$$\mu = \mu_o \exp(-\beta d) \qquad (8)$$

where μ_0 is coupling at zero edge-to-edge reactant separation and the decay constant β depends on the details of the structure through which tunnelling occurs. The decay constant has been reported by Chidsey as *ca.* 1.07 per CH_2 group for ferrocene alkane thiol monolayers on gold electrodes.[12]

k^o is given by Equation (6) or (7) for $\eta = 0$. Assuming values of two of the three parameters k^o, λ, or $\mu\rho$ fixes the value of the third. Figure 1 gives examples of reduction reaction rate constants calculated at different over-potentials from Equation (6) at 273K for a fixed value of k^o (1 s^{-1}) and a series of values of λ (and a corresponding series of $\mu\rho$ values). At small values of E - E°', these curves are the same as the exponentially increasing reaction

rates predicted by the Butler-Volmer Equation (4) for the same k^o value, but at larger over-potentials and at smaller values of λ, Equation (6) predicts reaction rates that increase less than exponentially with $E - E^{o\prime}$. At sufficiently large η, and/or small λ, the heterogeneous electron transfer rate constants fold over to become, at $\eta > \lambda$, essentially independent of over-potential. The heterogeneous electron transfer rates however do not decrease at $\eta > \lambda$, as predicted in homogeneous solutions in the classical Marcus "inverted" region, because of the continuum of electronic states in the metal electrode[6,8]. We will refer to Equations (6) and (7) as the heterogeneous Marcus equations, and to the range of over-potentials sufficiently large that rate constants lie substantially below those predicted by Butler-Volmer kinetics, eventually becoming independent of over-potential, as the Marcus-Density of States rate limited region (Marcus-DOS).

The limiting rate constants (at large η) in Figure 1 are determined by the value of $\mu\rho$, which in the series of calculations shown at constant k^o and decreasing λ, decreased in accord with λ.

Linear Sweep Voltammetry Calculations. Statements pertinent to calculating linear sweep voltammograms in which the reaction rate is controlled by either the Butler-Volmer Equations (4) and (5) or the heterogeneous Marcus Equations (6) and (7) are as follows: The current for first order reaction of a diffusionless electroactive species is

$$i_F = nFA\ (k_{Ox,\eta}\ \Gamma_{Red,\eta} - k_{Red,\eta}\ \Gamma_{Ox,\eta}) \qquad (9)$$

where the reaction rate constants are given by Equations (4,5) or (6,7), and F is the Faraday, A the electrode area, and $\Gamma_{Ox,\eta}$ and $\Gamma_{Red,\eta}$ the instantaneous surface coverages of the oxidized and reduced redox species, respectively. The applied potential, relative to $E^{o\prime}$, is η

$= \eta^* + \upsilon t$ where η^* is the initial potential, υ is potential sweep rate (V/s) and t is time. Overall chemical stability of Ox and Red is expressed in a mass balance equation

$$\Gamma^*_{Ox} + \Gamma^*_{Red} = \Gamma_{Ox,\eta} + \Gamma_{Red,\eta} = \Gamma \qquad (10)$$

where Γ is total surface coverage and the initial surface coverages Γ^*_{Ox} and Γ^*_{Red} are given by application of the Nernst equation.

Numerical solutions for linear sweep voltammetric currents were performed using a personal computer and a locally written program. To calculate voltammograms, η was changed in increments of $d\eta$ (< 1 mV, sufficiently small that calculated currents were independent of the chosen $d\eta$), allowing reaction to proceed during time intervals of $dt = d\eta/\upsilon$ at rates according to Equations (4,5) or (6,7). The instantaneous values of $\Gamma_{Ox,\eta}$ and $\Gamma_{Red,\eta}$ at each over-potential were calculated from their initial values and the oxidative or reductive charges passed since initiation of the potential sweep.

Behavior of "Marcus-DOS" Linear Sweep Voltammetry. Linear sweep voltammograms in which η approaches λ differ substantially from classical Butler-Volmer kinetics[2]. Figure 2 (lower) shows room temperature Butler-Volmer voltammograms calculated for several values of $\log[\upsilon/k^o]$ as the applied η is swept from 0.2 V to -1.0 V. (Increasing υ is completely equivalent to decreasing k^o in these calculations. Note that currents are normalized for surface coverage (Γ), electrode area, and sweep rate). At $\upsilon/k^o = 10^{-1}$, the voltammogram has an almost reversible shape. At larger values, $\upsilon/k^o = 1$, the peak currents become smaller and the wave broader, but at even larger ratios, no further change occurs. Larger sweep rates and smaller rate constants in Butler-Volmer kinetics simply cause the peak potential to shift to higher over-potentials.

Voltammograms like those in Figure 2 (lower) have been presented before[2,13], and are shown here simply for comparison to those calculated from the heterogeneous Marcus relations in Figure 2 (upper). Choosing a reorganizational energy λ = 0.85 eV (as was found for a ferrocene alkanethiol[6]), we see that as $\log[\upsilon/k^o]$ is increased, the 273K voltammetric peak potentials again move to larger over-potentials, but in addition the *waveshapes become progressively broader and the peak currents smaller*. The peak currents do not scale linearly with sweep rate as was the case in Figure 2 (lower), and they and the waveshape (*vide infra*) are quite sensitive to the value of λ.

The results of Figure 2 (upper) additionally show that significant changes in voltammetric behavior occur at over-potentials far less than the selected λ = 0.85eV; Marcus-DOS effects become apparent in the voltammetry in fact at over-potentials as small as *ca.* 30% of the chosen reorganizational energy. The curvature in Figure 1 is the qualitative reason for the voltammetric waveshapes changes in Figure 2 (upper); the incremental increase in reaction rate with increment in over-potential becomes smaller at larger over-potentials.

Figure 3 illustrates the sensitivity of voltammetric peak currents and waveshape to reorganizational energy, for the case of $\log[\upsilon/k^o]$ = 1. For decreasing λ (equivalently, as η/λ grows), the voltammetric peaks develop more prominent "diffusion-like" tails and the peak current falls. For very small λ values (0.10 eV, e.g., a reaction in a hydrocarbon-like solvent environment where the dipolar reorientation energies are small), the post-peak current tail can become so prominent that most of the total charge for consumption of Γ is passed in the post-peak region and the actual location of the peak potential becomes difficult to discern.

The latter effect places, in cases where $\eta/\lambda > 1$, a practical limitation on using ΔE_{PEAK} values for the purpose of determining k^o.

The E_{PEAK} values in Figure 3 vary somewhat with reorganizational energy, but these changes are relatively small compared to the dependence of ΔE_{PEAK} on $\log[\upsilon/k^o]$ shown in Figure 2 (upper). This important observation creates a framework for estimation of k^o values in the absence of information about the value of λ, as discussed below. Also note in Figure 3 that E_{PEAK}, as λ is decreased, first moves to more negative and then to more positive potentials. Normally, E_{PEAK} for reaction of a diffusionless electrochemical system occurs at an over-potential at which the rate of exhaustion of the reactant overtakes the exponential rise in rate constant. The peculiar reversal of the direction of change in E_{PEAK} in Figure 3 arises for small values of λ through the effect of limiting of rate constants at higher values of η/λ that occurs in the heterogeneous version of Marcus kinetics (e.g., Figure 1).

It is additionally apparent from Figure 3 that fitting of calculated to experimental voltammograms and/or the use of peak currents, should allow an evaluation of λ, the reorganizational energy. It is important to note that this application requires that all of the redox sites exhibit the same rate of reaction with the electrode. In experiments with ferrocene alkanethiols[14], at both room temperature in aqueous medium and low temperature in non-aqueous solvents, we typically observe dispersion (i.e., non-uniformity) in the value of the rate constant, by a factor of 3 or more. The dispersion is clearly evident, by non-linearities of ln[current] *vs.* time plots from potential step experiments. Such dispersion in non-aqueous systems has also been noted by Finklea[15]. Qualitatively, in potential sweep

experiments, the existence of a kinetic dispersion in which the rate constants among the population of redox sites vary from large to small is expected to produce a broadening and tailing of the voltammetric waves analogous to that seen in Figure 3. Additionally, apparent dispersions in rate constants can be induced (a) according to a plane-of-electron transfer model[16] in potential step experiments[17] through a variation in the couple's effective formal potential as a function of the Ox/Red ratio, and (b) simply by a distribution of actual $E^{o'}$ values among the surface redox sites because of how η is experimentally referenced to an average $E^{o'}$.[14b] Thus, application of waveshapes as in Figure 3 for assessment of reorganization energy requires that the absence of kinetic dispersion (from whatever source) be established beforehand by another method, of which potential step experiments would presently be the preferred approach. This is a limitation of the linear potential sweep method for measuring reorganizational energies.

Returning to the determination of rate constant k^o, Figure 4 gives working curves for the dependence of E_{PEAK} (*vs.* $E^{o'}$) on $\log[\upsilon/k^o]$ at 273K for Butler-Volmer (---) and for heterogeneous Marcus kinetics (——), based on various values of λ. Figure 5 similarly shows working curves for the dependence of normalized peak currents $i_p/\upsilon\Gamma A$ on $\log[\upsilon/k^o]$ at 273K. Figure 4 shows that for moderate values of over-potential (E_{PEAK} *vs.* $E^{o'}$), substantial deviations occur between calculations based on heterogeneous Marcus and on Butler-Volmer theories, the former predicting slower electron transfer kinetics. On the other hand, there are relatively minor differences between E_{PEAK} values calculated (at a given $\log[\upsilon/k°]$) for different reorganizational energies, until very large E_{PEAK} over-potentials are reached, whereupon E_{PEAK} values fold over toward values independent of the υ/k_o ratio. (This folding

over represents the approach to the plateau-like voltammetry seen at the bottom of Figure 3, and so will be difficult to explore since the E_{PEAK} becomes difficult to define.) The most significant observation to be made from Figure 4 is that, for moderate over-potentials, at which clearly defined peaks can be seen, the value of k^o that is obtained from an E_{PEAK} determination does not depend strongly on the selected value of reorganizational energy. This is the basis for our statement that the linear potential sweep method allows estimation of reaction rate constants, independent of knowledge of λ (or of models for its determination).

Figure 5, the analog of Figure 4, is based on the peak current dependence of $\log[\upsilon/k^o]$. A great sensitivity to the value of reorganizational energy is evident, and in the absence of kinetic dispersion (*vide supra*), peak currents can serve as a basis for measurement of reorganizational energy.

Tables I and II provide a more extensive numerical display of the peak potential and current dependencies on υ/k^o, and allow an expanded scale reconstruction of the 273K working curves of Figures 4 and 5.

Comparisons to Experimental Results. The electron transfer rate constant and reorganizational energy for the $CpFeCp^{0/+}$ reaction in aqueous $HClO_4$ at 273K in a mixed monolayer self-assembled by co-chemisorption of $CpFeCpCO_2(CH_2)_{18}SH$ and $CH_3(CH_2)_{17}SH$ on a Au(111) electrode have been determined[12] to be $k^o = 0.075 \pm 0.015\ s^{-1}$ and $\lambda = 0.85 \pm 0.05$ eV, respectively. These results were obtained using the potential step method.

Figure 6 (upper) shows the reduction scan part of a linear sweep voltammogram taken for a film of the above composition prepared as in the previous report[6]. This film contained $\Gamma = 8.8 \times 10^{-11}$ mol/cm^2 of ferrocenium sites and from potential step results was known to be

kinetically monodisperse. Overlaid on these data are voltammograms calculated (——) as outlined above using the kinetic parameters $k^o = 0.08\ s^{-1}$ and $\lambda = 0.85$ eV. To compare to the experimental data, which are uncorrected for charging current background, a double layer capacitance component is added to the theoretical curve. The double layer component was calculated by assuming that capacitance scales linearly with the mole fraction of oxidized ferrocene sites between limiting values of fully oxidized (5.14×10^{-7} F cm^{-2}) and fully reduced (8.7×10^{-7} F cm^{-2}) films. The fit between the experimental and calculated curves, for both potential sweep rates, is excellent, showing that assessment of k^o and λ by linear sweep voltammetry and by the potential step method yield fully consistent results.

We now illustrate use of the working curve data in Figures (4,5) and Tables I,II. The reductive E_{PEAK} of the experimental 250 mV/s voltammogram in Figure 6 (upper) is -238 mV. Application of the E_{PEAK} *vs.* $\log[\upsilon/k^o]$ working curve in Figure 4 shows that for $\log[\upsilon/k^o] = 0.5$, every λ-dependent curve except $\lambda = 0.1$ eV predicts an E_{PEAK} within 10 mV of the experimentally observed value. This value of $\log[\upsilon/k^o]$ corresponds to a rate constant of $0.08 \pm 0.002\ s^{-1}$, the uncertainty representing the 10 mV variation. Application of the Figure 5 working curve (or Table II) for $i_p/\upsilon\Gamma A$ *vs.* $\log[\upsilon/k^o]$ to find λ proves to be less satisfactory. The experimental uncertainties in measuring i_p/v (with capacitative background correction) and Γ couple with the very steep dependence of $i_p/\upsilon\Gamma A$ *vs.* $\log[\upsilon/k^o]$ produce substantial uncertainty in the estimated λ; values ranging from 0.9 to over 1.1 eV can be obtained. Simulation of the entire current-potential curve as in Figure 6 seems to be more reliable for estimation of the reorganizational energy, than use of peak currents alone.

Figure 6 (lower) shows the best fit to the experimental curve with a calculated Butler-

Volmer voltammogram that we were able to obtain, using $\alpha = 0.5$, $k^o = 0.06\ s^{-1}$, and matching the E_{PEAK} values. The Butler-Volmer theory is much less successful in fitting to the experimental result than is the heterogeneous Marcus calculation; most significantly it was not possible to match the overall waveshape. The effects of the "DOS-limited" aspect of Marcus theory are clearly evident in this waveshape comparison, even though the over-potentials at the E_{PEAK} values in Figure 6 (upper) are much less than the obtained reorganizational energy. On the other hand, the k^o obtained from the poor fit ure 6 (lower) is not very different from that determined using heterogeneous Marcus kinetics, which is a reflection of the fact that in Figure 4 the lines for the two theories are not very different at E_{PEAK} = -238mV.

Figure 7 presents another somewhat more demanding comparison of the Figure 6 250 mV/s reductive voltammetric waveshape to theory. By calculating the current axis as $\log[i_\eta/nFA\Gamma_{ox,\eta}]$, which is equal to the rate constant $\log[k_{ox,\eta},]$ the data are transformed into a rate constant/over-potential curve which can be compared directly with curves like those in Figure 1. Figure 7 (--- • ---) corresponds to the heterogeneous Marcus case of $k^o = 0.08\ s^{-1}$ and $\lambda = 0.85$ eV, giving an excellent fit to the transformed voltammogram over the major portion of the wave, from -0.2 to -0.3V. The fit fails at the highest over-potentials where the small size of the experimental currents causes substantial uncertainty, and at the leading edge of the voltammogram owing to neglect in this plot of the pseudo-reversibility of the reaction at the lowest over-potentials.

Mixed $CpFeCpCO_2(CH_2)_{18}SH/CH_3(CH_2)_{17}SH$ films[18] like those used in Figures 6 and 7 exhibit highly linear plots of ln[transient current] *vs.* time in potential step

experiments. The slope of an ln[i] *vs.* t plot gives the reaction rate constant; the plot's linearity means that all of the ferrocene sites exhibit the same electron transfer rate constant. One infers that these ferrocene sites experience nearly identical dipolar environments and nearly identical distances and alkane layer structure intervening between ferrocene and gold surface. This behavior is a consequence of the high degree of ordering achieved in these films.

Other recent work[14b,15] has produced less ordered self-assembled monolayers on Au (111) and bulk gold that exhibit some curvature in potential step ln[i] *vs.* time plots for their electrochemical reactions. The voltammetric waves for these monolayers also are broadened even at slow potential scan rates (near-equilibrium). These films have some dispersion in either the dipolar environments of the redox sites, or in the structure of the alkane layer tunnelling barrier, or both, which gives rise to a range of apparent formal potentials and/or of electron transfer rate constants for the immobilized redox sites (*vide supra*). Dispersion in rate constants is in fact well-known in solid state electron transport in amorphous films[19], where dispersions in site dipolar environment, intersite distance, etc, occur in the material's preparation and are thereafter fixed by the sites' limited mobilities. Kinetic dispersion is found for example in electron transport through dry, mixed valent films of poly-vinylferrocene.[20] The kinetic dispersion in the self-assembled ferrocene alkanethiol films can then be regarded as an example of two-dimensional disorder. We will apply the heterogeneous Marcus theory to voltammograms of such monolayers.

Figure 8 (inset) shows an experimental voltammogram at 298K in 1 M $HClO_4$ for a ferrocene alkanethiol monolayer based on co-chemisorbed $CpFeCpCO_2(CH_2)_{16}SH$ (3.6 x 10^{-}

^{10} mol/cm^2) and $CH_3(CH_2)_{15}SH$. The bold curve in Figure 8 is the background-corrected reductive branch and the curve ---o--- is a voltammogram calculated from heterogeneous Marcus theory for $k^o = 1.0\ s^{-1}$ and $\lambda = 0.85$ eV. The theoretical curve was chosen for the best fit to the E_{PEAK} *vs.* $E^{o\prime}$ value. The match between the experimental and calculated voltammetric waveshapes is not very good; the experimental voltammogram is broader and exhibits a lower peak current. The monolayer sample used in Figure 8 gave for a potential step to $E^{o\prime}$ from a potential off the wave, ln[i] *vs.* t plots with slopes indicating a rate constant of *ca.* 4.5 s^{-1} at times before ca. 50 msec. The slope decreased to a value of about 1 s^{-1} at about 100 msec, remaining reasonably constant thereafter out to 1.9 sec, at which point 51% of the ferrocene sites had been oxidized and the reaction was complete. The dispersion in the ferrocenium sites' rate constants is thus roughly 5-fold and is the presumed source of the peak broadening seen in Figure 8.

Voltammograms of the film in Figure 8, taken for a series of potential scan rates produced the E_{PEAK} - $E^{o\prime}$ values (■) plotted in Figure 9 against log[υ]. Figure 9 contains overlays of the experimental plot with curves from Figure 4 to produce a good match[21] of the variation of E_{PEAK} with scan rate. Butler-Volmer kinetics (--- + ---) fail to describe the observed peak potential-scan rate dependence in Figure 9. The heterogeneous Marcus fit corresponds to a rate constant $k^o = 1\ s^{-1}$ which is close to that obtained, 1.25 s^{-1}, by the potential step method for the same chain length ferrocene alkanethiol monolayer chemisorbed in a highly ordered film[6] like that in Figures 6,7. That is, the linear sweep voltammetry electron dynamics analysis of a film with a significant kinetic dispersion, gives an "average" k^o that is a reasonable estimate of the value in a kinetically uniform film. This observation is

important in a practical sense, showing that determinations of "average" kinetic rates by comparisons like those in Figures 8,9 can be relatively forgiving with respect to the degree of film disorder. The extent to which more substantial kinetic dispersion may induce drift of the "average k^o" away from that appropriate for a kinetically uniform monolayer will require further experience to evaluate.

Figures 10 and 11 show voltammetric results for another example of a kinetically disperse $CpFeCpCO_2(CH_2)_{16}SH$:$CH_3(CH_2)_{15}SH$ monolayer on a 0.5 mm dia. etched Au electrode, in 2:1 EtCl:PrCN at 150K. Figure 10 shows the determination of k^o and λ by a method analogous to that described above, using a set of calculations like those in Figure 4, but for 150K. The experimental data for $E_{PEAK} - E^{o\prime}$ are plotted against log[v] and compared to the corresponding 150K working curves. The working curves exhibit a greater variation with reorganizational energy at this low temperature than they do at room temperature; this and the substantial experimental potential sweep rate range allows in this case making an estimate of λ as shown by the best match. The results indicate λ = 0.9 to 1.0 eV and $k^o = 1.4(\pm 0.4)\times 10^{-4}$ s^{-1}; the error in k^o represents 2 standard deviations. These results are consistent with a large body of unpublished data[14b] that we have obtained at low temperatures in this solvent.

The waveshape of the low temperature voltammetry is examined in Figure 11, which displays the effects of the kinetic dispersion (or equivalently, in $E^{o\prime}$) in these films. Figure 11A (solid squares) shows a background corrected 100 mV/s voltammogram for the $CpFeCpCO_2(CH_2)_{16}SH$:$CH_3(CH_2)_{15}SH$ monolayer ($\Gamma = 1.5\times 10^{-10}$ mol/cm^2) at 150K. The open squares represent an attempted fit of this voltammogram using λ = 0.4 eV and

$k^o = 5x10^{-4}\ s^{-1}$. We believe that the low value of λ in this fit is an artifact, caused by the voltammetric peak broadening and tailing of the kinetic dispersion. A potential step experiment on this film exhibited a 7-fold slope variation in a ln[i] *vs.* t plot. Figure 11B compares the experimental voltammetry to a voltammogram calculated for the results obtained in Figure 10, i.e., λ = 0.9 to 1.0 eV and $k^o = 1.4(\pm 0.4)x10^{-4}\ s^{-1}$. The E_{PEAK} value matches exactly, but the waveshapes are quite different. The difference reflects the effects of the dispersion in kinetic behavior of the ferrocene sites in this film.

ACKNOWLEDGEMENTS

This research was funded in part by grants from the Office of Naval Research and the National Science Foundation. The authors gratefully acknowledge helpful discussions and experimental data for Figures 6 and 7 which were provided by C.E.D. Chidsey and M. Linford of Stanford University. Roger Terrill of UNC-CH is gratefully acknowledged for assistance with data analysis.

References

1. Nicholson, R. S., Shain, I.; *Anal.Chem.* **1964**, *36*, 706.
2. Laviron, E.; *J. Electroanal. Chem.* **1979**, *101*, 19.
3. Bard, A. J.; Faulkner, L. R.; *Electrochemical Methods*; Wiley: New York, 1980.
4. Marcus, R. A.; *J. Chem Phys.* **1965**, *43*, 679.
5. Newton, M. D.; Sutin, N.; *Annu. Rev. Phys. Chem.* **1984**, 35, 437.
6. Chidsey, C. E. D.; *Science* **1991**, *251*, 919.
7. Finklea, H. O.; Hanshaw, D. D.; *J. Am Chem. Soc.* **1992**, 114, 3173.
8. Hummel, R. E.; *Electronic Properties of Materials*: Springer-Verlag: Berlin, 1985.

9. Chidsey, C. E. D.; Bertozzi, C. R.; Putvinski, T. M.; Mujsce, A. M. *J. Am. Chem. Soc.* **1990**, *112*, 4301.

10. Creager, S.E.; Hockett, L. A.; Rowe, G. K. *Langmuir* **1992**, *8*, 854.

11. Curtin, L.J.; Peck, S.R.; Tender, L.M.; Murray, R.W.; Rowe, G.K.; Creager, S.E. *Anal. Chem.* **1993**, *65*, 386.

12. Dubois, L.H.; Nuzzo, R. G. *Annu. Rev. Phys. Chem.* **1992**, *43*, 437.

13. Hubbard, A.T.; Anson, F. in Bard, A.J. (Ed.) *Electroanalytical Chemistry*, Vol. 4, Marcel Dekker: NY, pp. 129.

14. a) Peck, S. R. *Ph. D. Dissertation*, University of North Carolina, 1992. b) Tender, L.M.; Carter, M. T.; Richardson, J. N.; Rowe, G. K.; Murray, R. W.; University of North Carolina, unpublished results.

15. Ravenscroft, M. S.; Finklea, H. O. *J. Phys. Chem.*, **1994**, *98*, 3843.

16. Smith, C. P.; White, H. S. *Anal. Chem.* **1992**, *64*, 2398.

17. Creager, S. E.; Weber, K. *Langmuir*, **1993**, *9*, 844.

18. Chidsey, C. E. D.; Holcolm, M.; Stanford University, 1993, *unpublished results.*

19. a) Scher, H.; Montroll, E.W.; *Phys. Rev. B* **1975**, *12*, 2455. b) Pfister, G. *Phys. Rev. B* **1977**, *16*, 3676.

20. Sullivan, M. G., Murray, R. W. *J. Phys. Chem.*, **1994**, *98*, 4343.

21. The comparison ignores the difference between experimental (298K) and calculated (273K) temperatures; the error is between 20 and 33% in the fitted valve of k°.

FIGURE LEGENDS

Figure 1. Calculated $\log(k_{red,\eta})$ *vs.* over-potential (η=E-E$^{o\prime}$) at 273K and k^o = 1.0 s^{-1}, based on heterogeneous Marcus kinetics (——) top-to-bottom λ = 1.00, 0.9, 0.8, 0.7, 0.6, 0.5, 0.4, 0.3, 0.2, and 0.1 eV. - - - - is Butler Volmer calculation for k^o = 1.0 s^{-1} and α = 0.5.

Figure 2. Calculated, normalized voltammetric waves based on (lower, α=0.5) Butler-Volmer kinetics and (upper, λ=0.85 eV) heterogenous Marcus kinetics, at 273K, for left-to-right values of $\log[\upsilon/k^o]$ = -1, 0, 1, 2, and 3.

Figure 3. Dependence of calculated, normalized voltammetric waveshape on reorganization energy λ, based on heterogeneous Marcus kinetics, T = 273 K; $\log[\upsilon/k^o]$ = 1.0. Top-to-bottom λ =1.00, 0.9, 0.8, 0.7, 0.6, 0.5, 0.4, 0.3, 0.2, and 0.1 eV. Bars mark E_{PEAK} values.

Figure 4. Working curves of voltammetric E_{PEAK} over-potentials *vs.* $\log[\upsilon/k^o]$, ratio of potential sweep rate to electron transfer rate constant. —— heterogeneous Marcus kinetics for top-to-bottom, λ = 1.00, 0.9, 0.8, 0.7, 0.6, 0.5, 0.4, 0.3, 0.2, and 0.1 eV; - - - - Butler-Volmer kinetics for α=0.5.

Figure 5. Working curves of normalized peak currents *vs.* $\log[\upsilon/k^o]$, ratio of potential sweep rate to electron transfer rate constant. —— heterogeneous Marcus kinetics for top-to-bottom, λ = 1.00, 0.9, 0.8, 0.7, 0.6, 0.5, 0.4, 0.3, 0.2, and 0.1 eV; - - - - Butler Volmer kinetics for α=0.5.

Figure 6. (top panel) Comparison of scan rate-normalized experimental (noisy line) and (——), heterogeneous Marcus voltammetry calculated for k^o = 0.08 s^{-1}, λ = 0.85 eV, T =

273K. Experimental voltammogram is for well ordered, kinetically uniform, mixed self-assembled monolayer of $CpFeCpCO_2(CH_2)_{18}SH$ (Γ = 9.3(±-.2)x10^{-11} mol/cm^2) and $CH_3(CH_2)_{17}SH$ co-chemisorbed on Au(111), T = 273K, A = 0.7 cm^2, υ = 100 mV/s (left-hand-curve) and 250 mV/s (right-hand-curve), 0.1M $HClO_4$. Experimental currents at η = -0.5 V and 0.2 V (at both scan rates) give double-layer capacitances of 5.4x10^{-7} F and 8.7x10^{-7} F at these potential limits, which are used to simulate capacitance background of calculated voltammogram. **(lower panel)** Comparison of scan rate-normalized experimental (noisy line, same as 250mV/s experiment in upper panel) and (——), Butler-Volmer voltammetry calcualted for k^o = 0.06 s^{-1}, α = 0.5, T = 273K.

Figure 7. Reduction branch of 250 mV/s experimental voltammogram (noisy curve) of Figure 6(upper) with current axis transformed as $\log[i_\eta/nFA\Gamma_{ox,\eta}] = k_{ox,\eta}$, compared to curves calculated as in Figure 1 for (---•---) heterogeneous Marcus kinetics with k^o = 0.08 s^{-1}, λ = 0.85 eV, T = 273K and (--- + ---) Butler-Volmer kinetics with k^o = 0.08 s^{-1} and α = 0.5 Inset shows complete experimental cyclic voltammogram for 250 mV/s.

Figure 8. Reduction branch (——) of 10 V/s experimental voltammogram (entire voltammogram shown in inset) for a disordered, kinetically disperse, mixed self-assembled monolayer of $CpFeCpCO_2(CH_2)_{16}SH$ (Γ = 3.6x10^{-10} mol/cm^2) and $CH_3(CH_2)_{15}SH$ co-chemisorbed on etched Au, T = 298K, A = 0.03 cm^2, 1.0 M $HClO_4$. Double layer, background-subtracted voltammogram (——) is compared to voltammogram calculated (---•---) for heterogeneous Marcus kinetics with k^o = 1.0 s^{-1}, λ = 0.85 eV, T = 273K, best fit for E_{PEAK} value.

Figure 9. Over-potentials (■, see table inset, $E_{PEAK} - E^{o\prime} = 0.5\Delta E_{PEAK}$) for monolayer

described in Figure 8. Voltammograms taken as a function of potential scan rate from 50 mV/s to 50 V/s, experimental data (■) positioned on log[υ/k^o] axis for k^o = 1.0 s^{-1}. (——) curves from Figure 4; λ varies from top-to-bottom as in Figure 4; experimental k^o = 1.0 s^{-1} was selected for best fit of experimental data with Figure 4 curves. (— + —) Butler-Volmer curve from Figure 4.

Figure 10. λ-dependent working curves for peak over-potential (E_{PEAK}-E°′) *vs.* log ($\upsilon/k°$) at 150K, compared to data (squares) for a monolayer of $CpFeCpCO_2(CH_2)_{16}SH$: $CH_3(CH_2)_{15}SH$ (Γ=1.5x10^{-10} mol/cm^2) in 2:1 EtCl:PrCN with 0.075M Bu_4NPF_6 electrolyte. The data fit best to the working curves using $k°$ = 1.4 x 10^{-4} s^{-1} and λ=0.9 eV.

Figure 11. Comparison of Marcus-DOS theory to oxidation branch of cyclic voltammogram at 150K. Experimental details are the same as Figure 10. Panel A: best fit of waveshape at 100 mV/s by heterogeneous Marcus theory, for λ=0.4 eV and $k°$= 5x10^{-4} s^{-1}; Panel B: comparison of 100 mV/s waveshape to heterogeneous Marcus theory, for λ=0.9 eV and $k°$ = 1.4x 10^{-4} s^{-1}. Calculated and experimental voltammograms are denoted by solid lines, and open circles, respectively.

Table I. Calculated values of over-potential E_{PEAK} - E°′, in mV, as a function of reorganization energy, λ and log (v/k°).

Log (v / k°)	Reorganizational Energy (eV)										Butler-Volmer
	0.1	0.2	0.3	0.4	0.5	0.6	0.7	0.8	0.9	1	
-4	0	0	0	0	0	0	0	0	0	0	0
-3.5	0	0	0	0	0	0	0	0	0	0	0
-3	1	0	0	0	0	0	0	0	0	0	0
-2.5	2	2	2	2	2	2	2	3	3	3	3
-2	7	7	7	7	7	7	7	7	8	7	8
-1.5	19	20	20	20	20	20	20	20	21	20	20
-1	44	48	48	48	48	49	49	49	50	49	50
-0.5	88	96	96	96	97	97	98	98	97	98	95
0	148	162	163	163	162	162	162	162	162	162	153
0.5	210	243	246	243	240	237	235	232	232	229	213
1	267	327	343	337	327	321	316	310	308	306	270
1.5	313	402	443	445	432	418	408	397	391	386	330
2	354	464	534	561	553	532	513	497	483	475	390
2.5	389	516	607	664	680	664	637	610	591	574	448
3		561	669	748	794	804	780	745	713	686	507
3.5		605	726		888	926	931	899	856	818	560
4		642	772		966	1026	1050	1037	1023	971	625
4.5			818		1034	1109	1100	1193	1188	1147	685
5					1093	1182	1255	1285	1328	1320	743
5.5					1147	1247	1331	1398			803
6					1196	1309	1401	1479			863

Table II. Calculated values of normalized peak current, $i_{PEAK}/v\Gamma A$ (C $mol^{-1}v^{-1}$) as a function of organizational energy, λ, and log(υ/k°).

Log (υ / k°)	Reorganizational Energy (eV)										Butler - Volmer
	0.1	0.2	0.3	0.4	0.5	0.6	0.7	0.8	0.9	1	
-4	-939287	-938974	-938974	-938974	-938974	-938974	-938974	-938974	-938974	-938974	-939600
-3.5	-939287	-938974	-938974	-938974	-938974	-938974	-938974	-938974	-938974	-938974	-939700
-3	-939287	-938869	-938869	-938869	-938869	-938869	-938869	-938869	-938869	-938869	-939400
-2.5	-939287	-938243	-938243	-938347	-938347	-938347	-938347	-938347	-938347	-938347	-939100
-2	-939287	-932814	-932814	-932918	-933023	-933127	-933127	-933127	-933127	-933232	-933600
-1.5	-892933	-897631	-897631	-898571	-899197	-899615	-899928	-900241	-900450	-900554	-900600
-1	-762224	-789682	-789682	-795110	-798660	-801270	-803149	-804715	-805064	-806908	-813600
-0.5	-554886	-643522	-643522	-661165	-672962	-681314	-687578	-692485	-696452	-699689	-730400
0	-342954	-513752	-513752	-551336	-576288	-594036	-607295	-617526	-625774	-632351	-698800
0.5	-170068	-295139	-389099	-450904	-492559	-522209	-544237	-561254	-574722	-585580	-692100
1	-67923	-155243	-258912	-343894	-404759	-448502	-480971	-505818	-525445	-541210	-691000
1.5	-23761	-64822	-139270	-229680	-308189	-367801	-412276	-446310	-473141	-494647	-690900
2	-7813	-23187	-59143	-124027	-204937	-278435	-336586	-381373	-416452	-444535	-690900
2.5	-2508	-7697	-21360	-52858	-110038	-183431	-252961	-309650	-354438	-390143	-690900
3	-804	-2478	-7118	-19126	-46656	-97259	-164534	-230411	-285847	-330426	-690900
3.5	-256	-789	-2296	-6380	-16829	-40820	-85890	-147517	-210366	-264445	-690900
4	-81	-250	-731	-2058	-5608	-14637	-35465	-75252	-132066	-192096	-690800
4.5	-26	-79	-232	-655	-1808	-4866	-12622	-30621	-65793	-117972	-690800
5	-8	-25	-73	-208	-576	-1567	-4181	-10805	-26290	-50516	-690700
5.5	-3	-8	-23	-66	-182	-499	-1345	-3566	-9424	-23480	-690700
6	-1	-3	-7	-21	-58	-158	-428	-1145	-3165	-8003	-690800

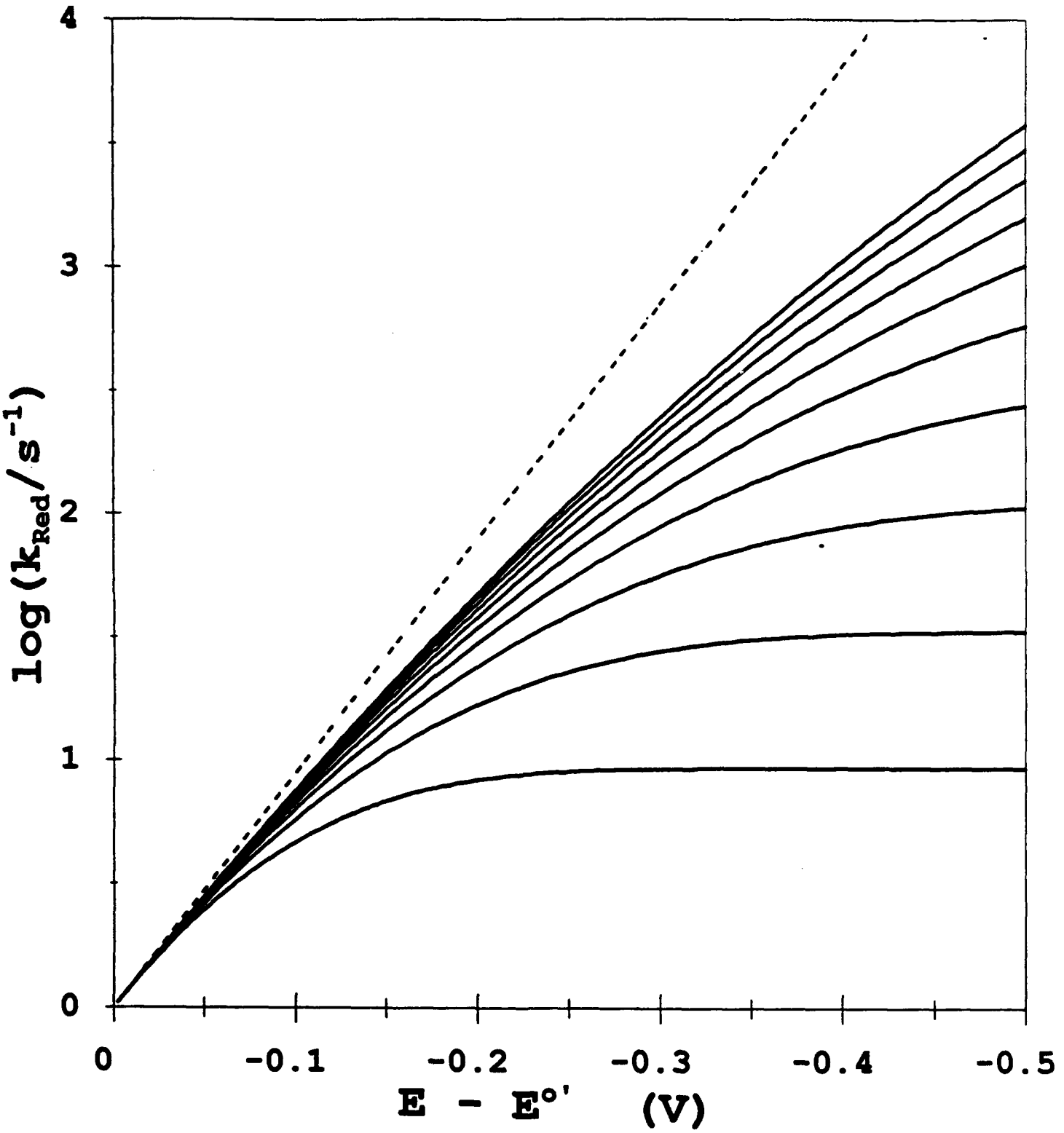

Fig 1

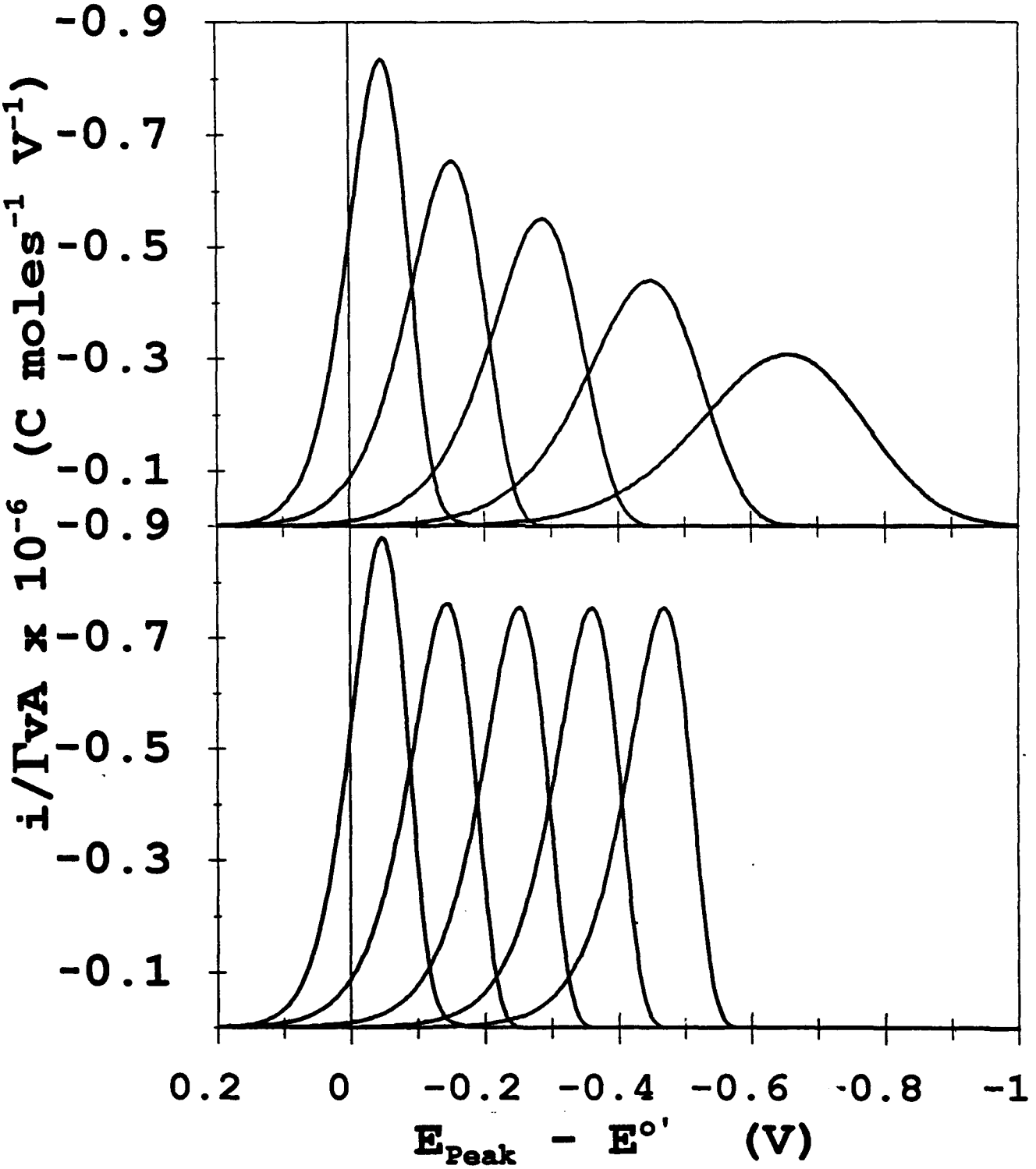
-0.9
-0.7
-0.5
-0.3
-0.1
-0.9
-0.7
-0.5
-0.3
-0.1
i/ΓvA x 10⁻⁶ (C moles⁻¹ V⁻¹)
0.2
0
-0.2
-0.4
-0.6
-0.8
-1
E_Peak - E°' (V)

Fig 2

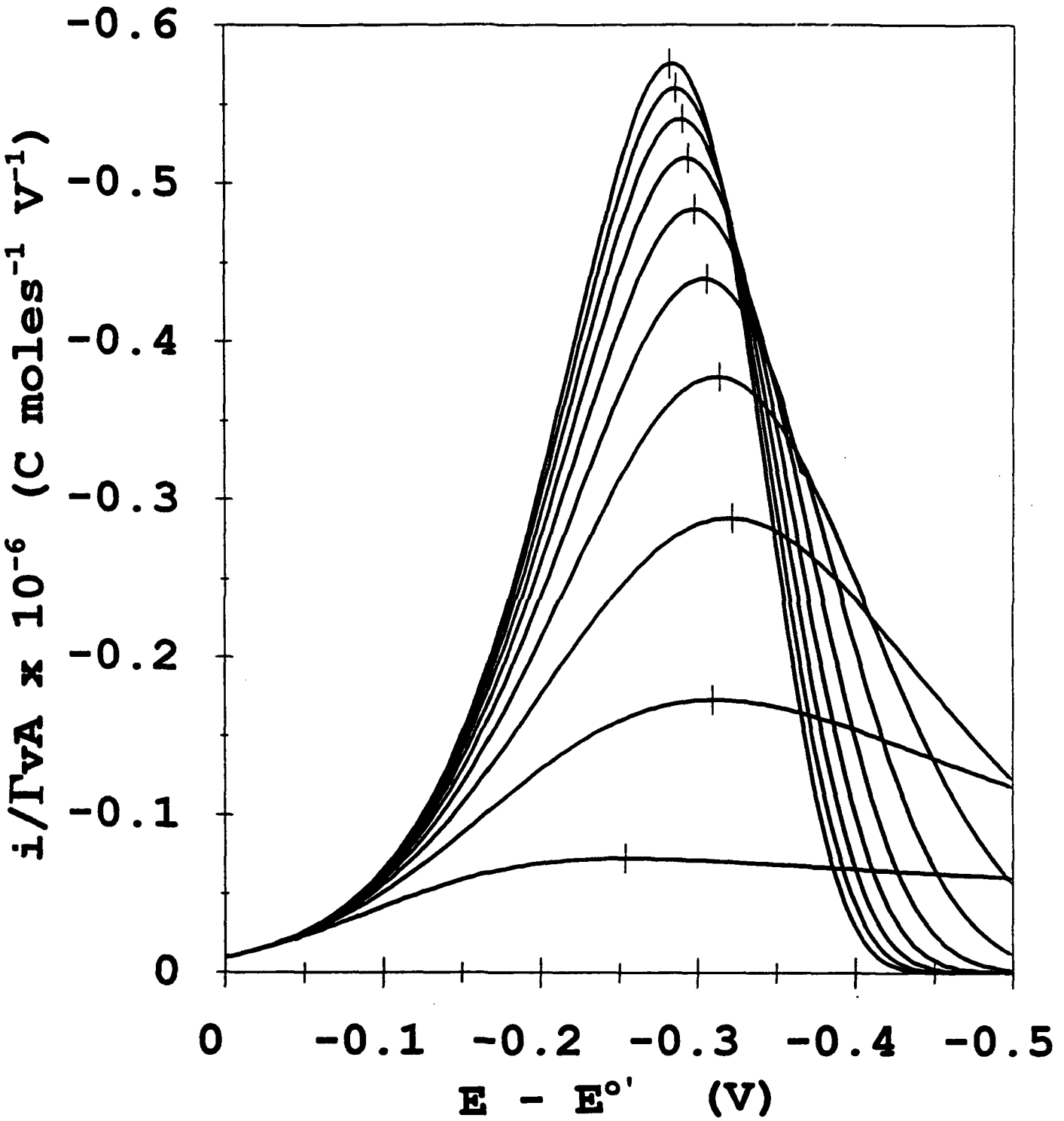

Fig. 3

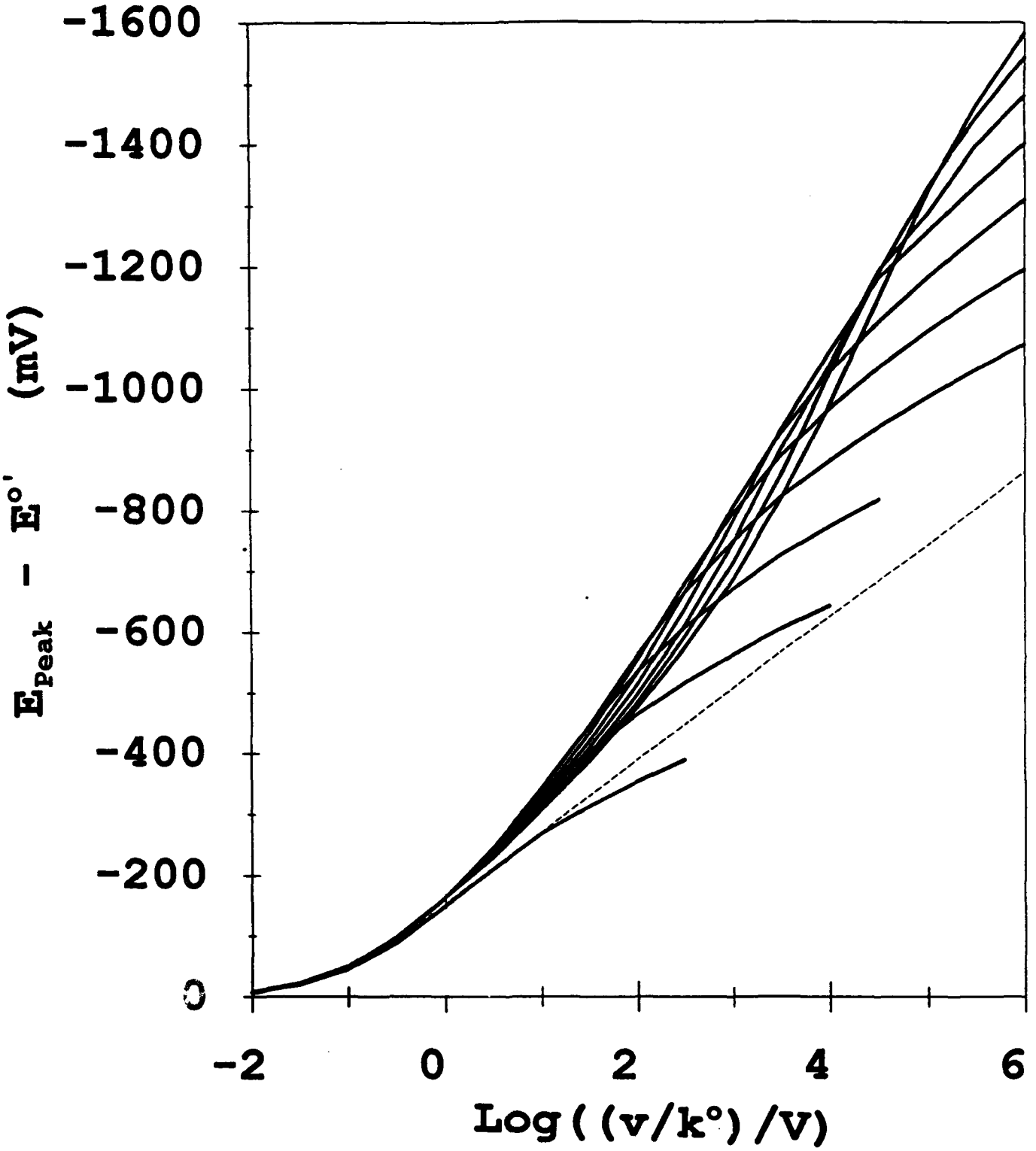

Fig. 4

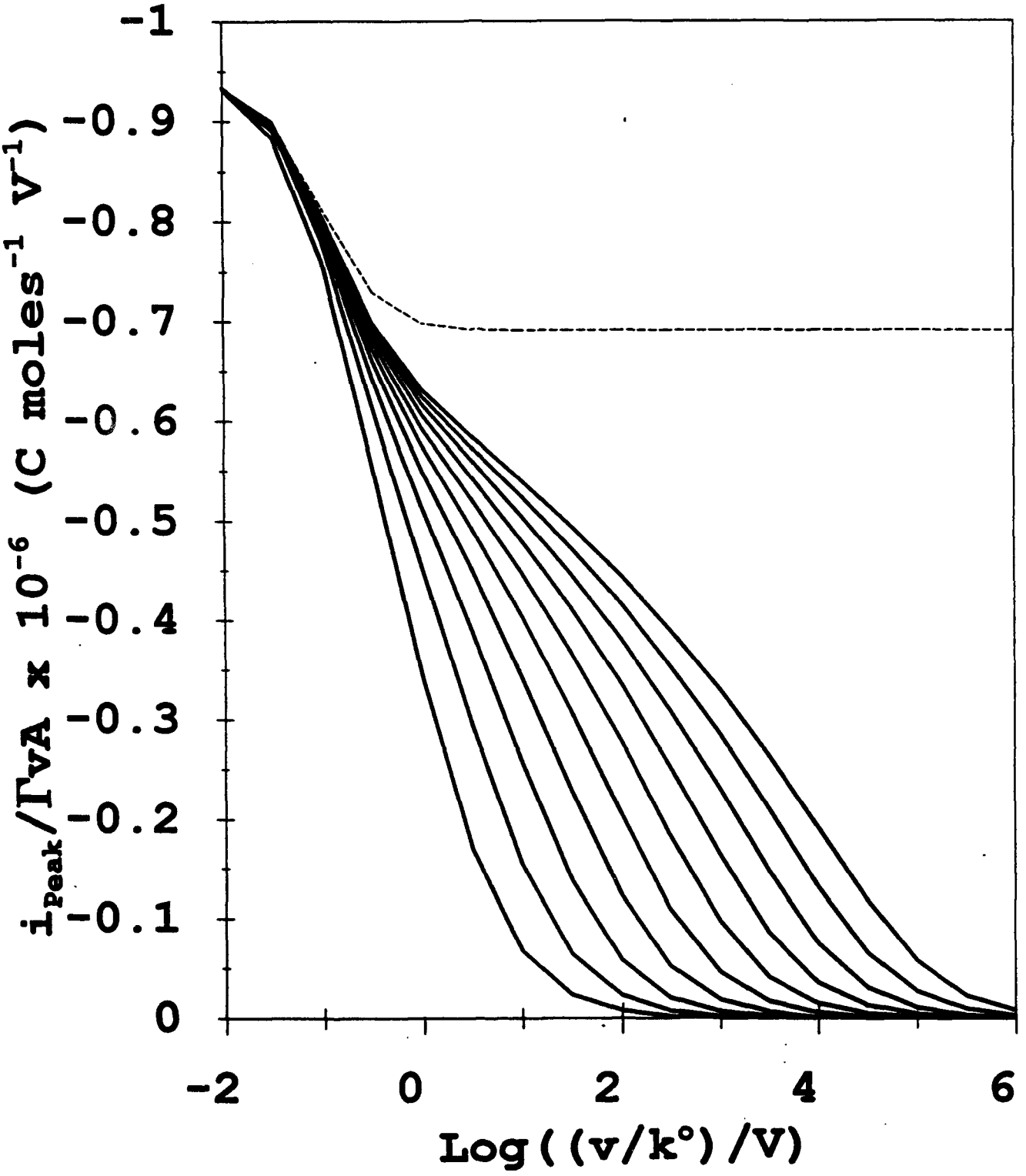
-1
-0.9
-0.8
-0.7
-0.6
-0.5
-0.4
-0.3
-0.2
-0.1
0
$i_{Peak}/\Gamma vA \times 10^{-6}$ (C moles^{-1} V^{-1})
-2
0
2
4
6
Log ((v/k°) /V)

Fig. 5

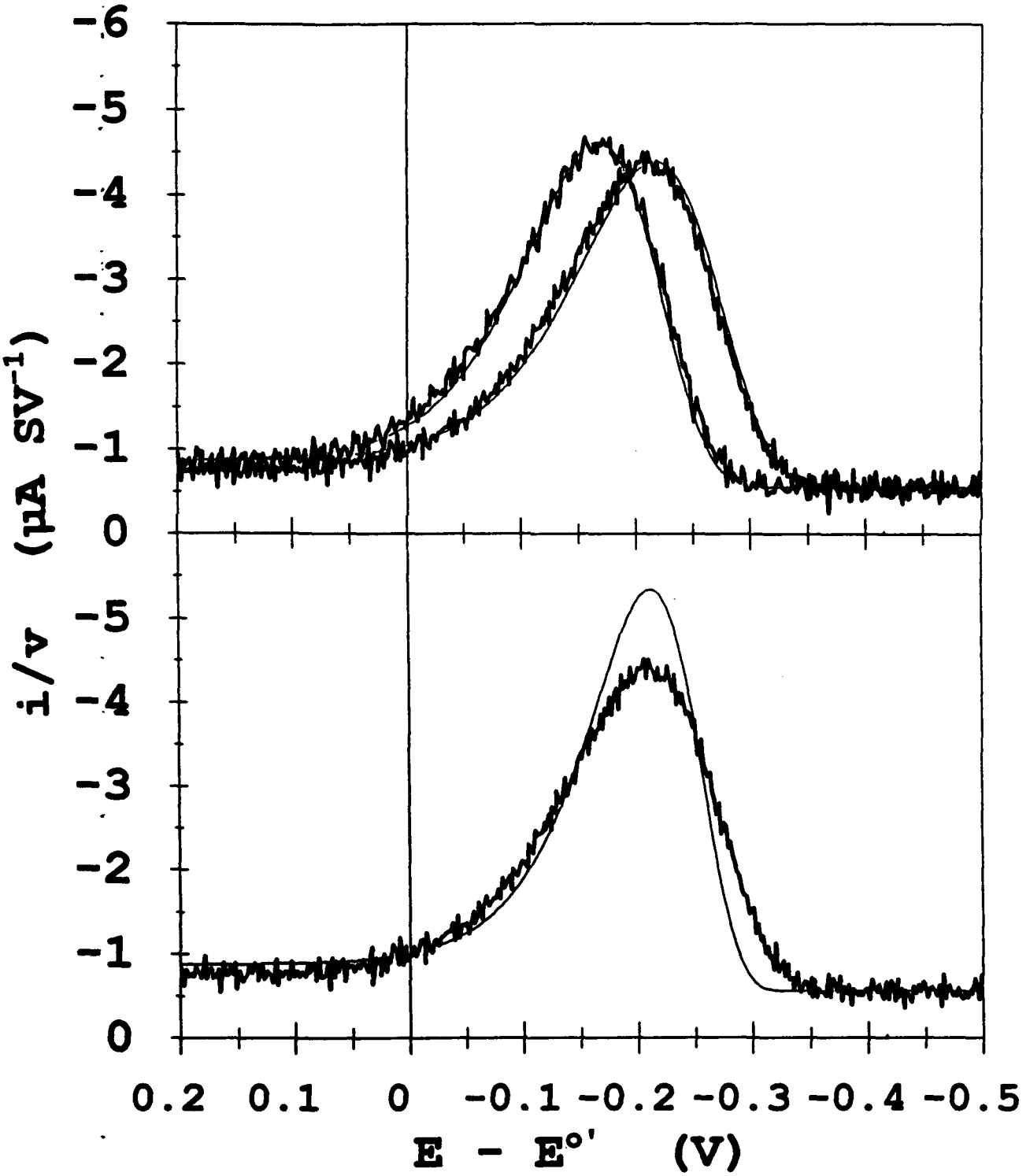

Fig. 6

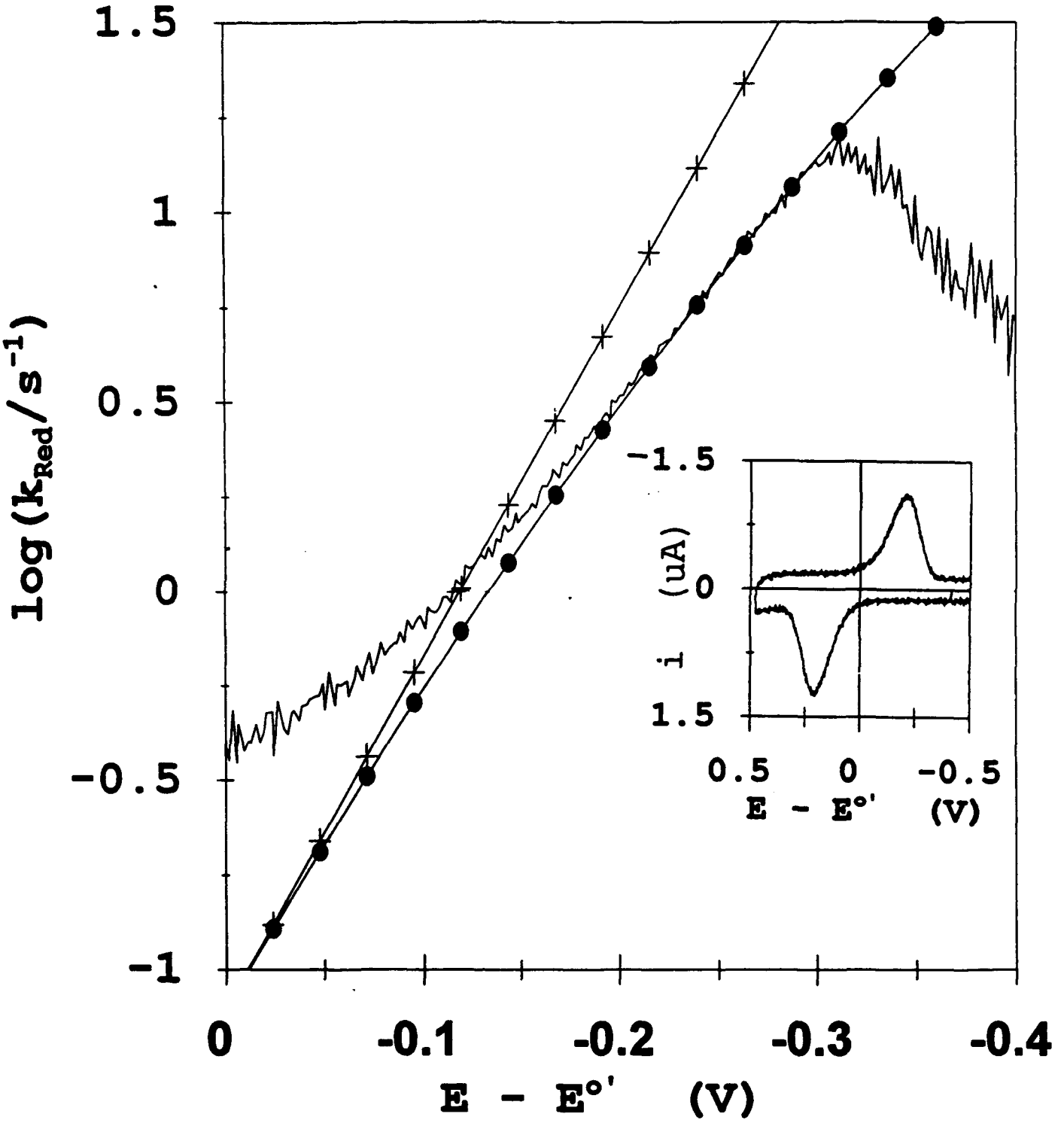

Fig 1

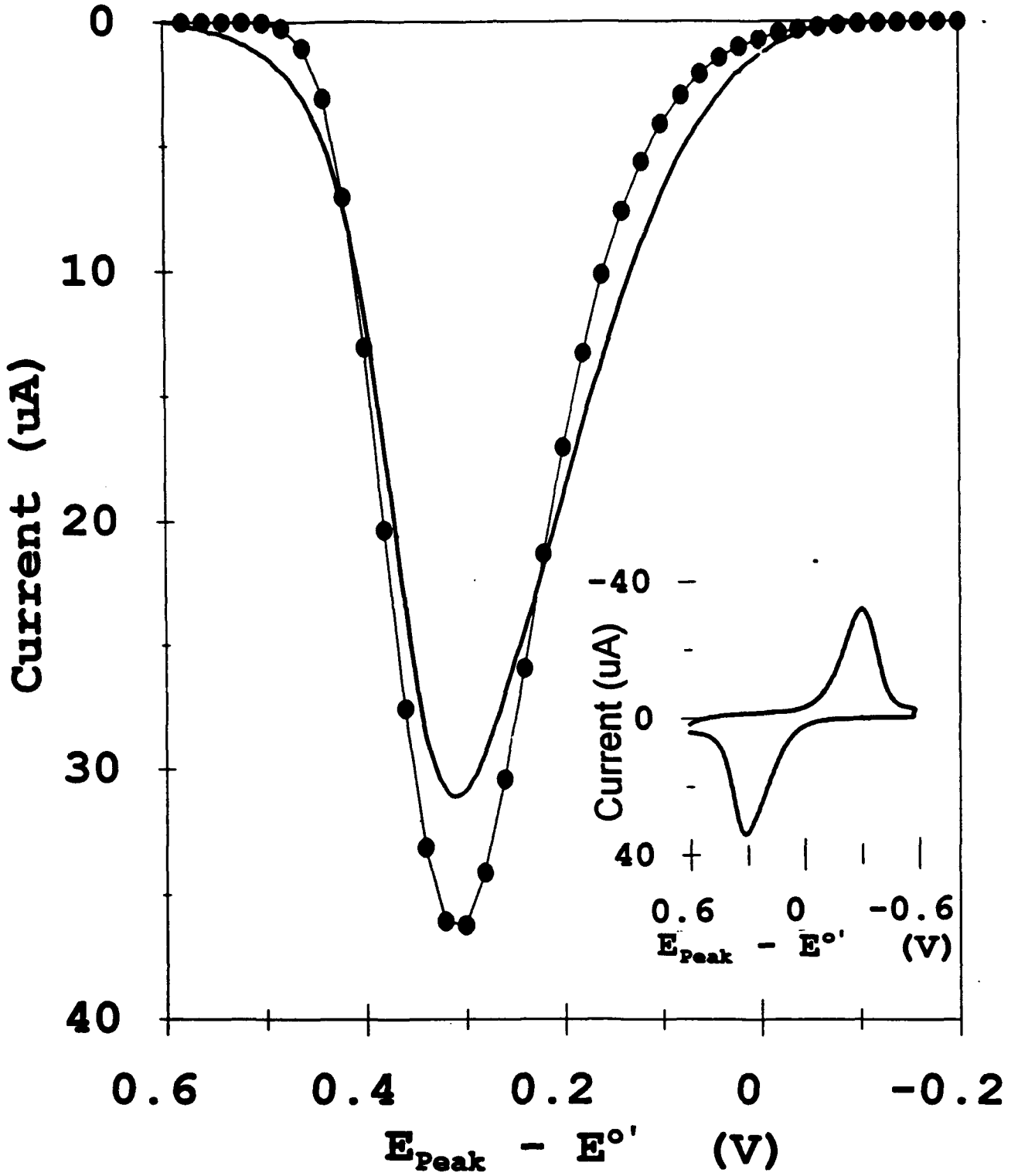
0
10
20
30
40
Current (uA)
0.6
0.4
0.2
0
-0.2
E Peak - E°' (V)
-40
0
40
Current (uA)
0.6
0
-0.6
E Peak - E°' (V)

Fig. 8

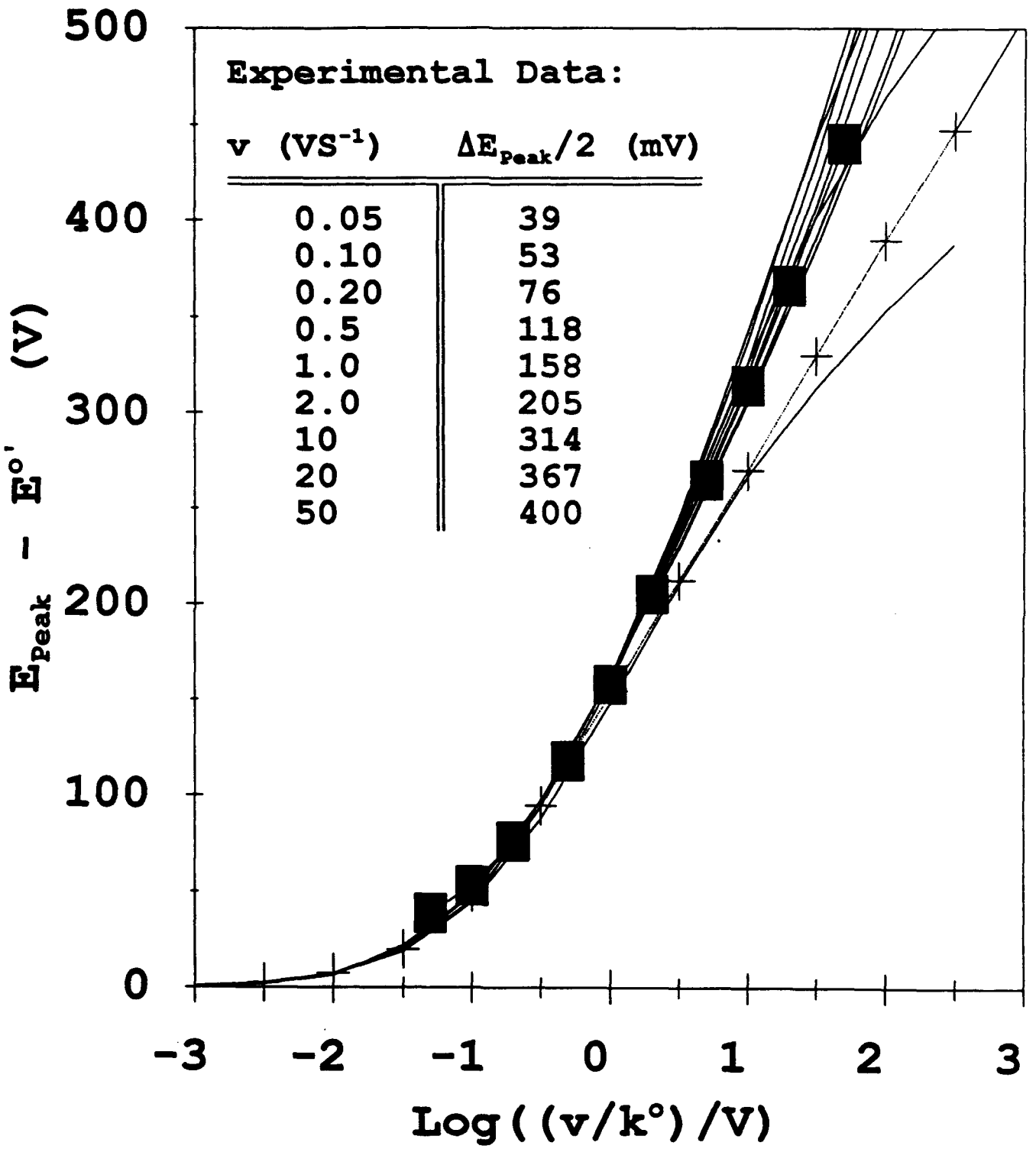
Experimental Data:
v (VS-1) ΔEPeak/2 (mV)
0.05 39
0.10 53
0.20 76
0.5 118
1.0 158
2.0 205
10 314
20 367
50 400
500
400
300
200
100
0
EPeak - E°' (V)
-3
-2
-1
0
1
2
3
Log((v/k°)/V)

Fig 9

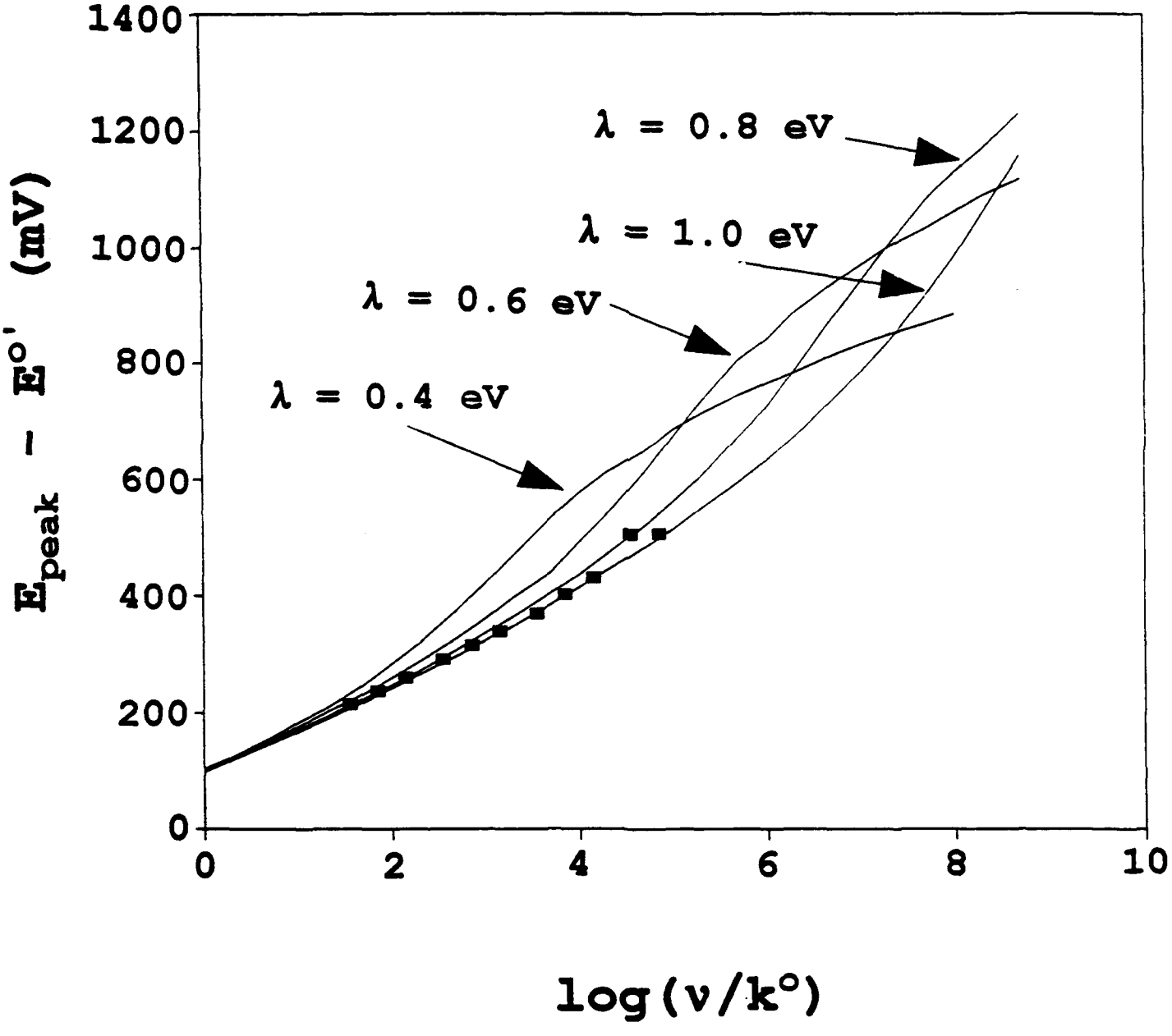
1400
1200
1000
800
600
400
200
0
0
2
4
6
8
10
λ = 0.8 eV
λ = 1.0 eV
λ = 0.6 eV
λ = 0.4 eV
E_peak - E°' (mV)
log(v/k°)

Fig 10

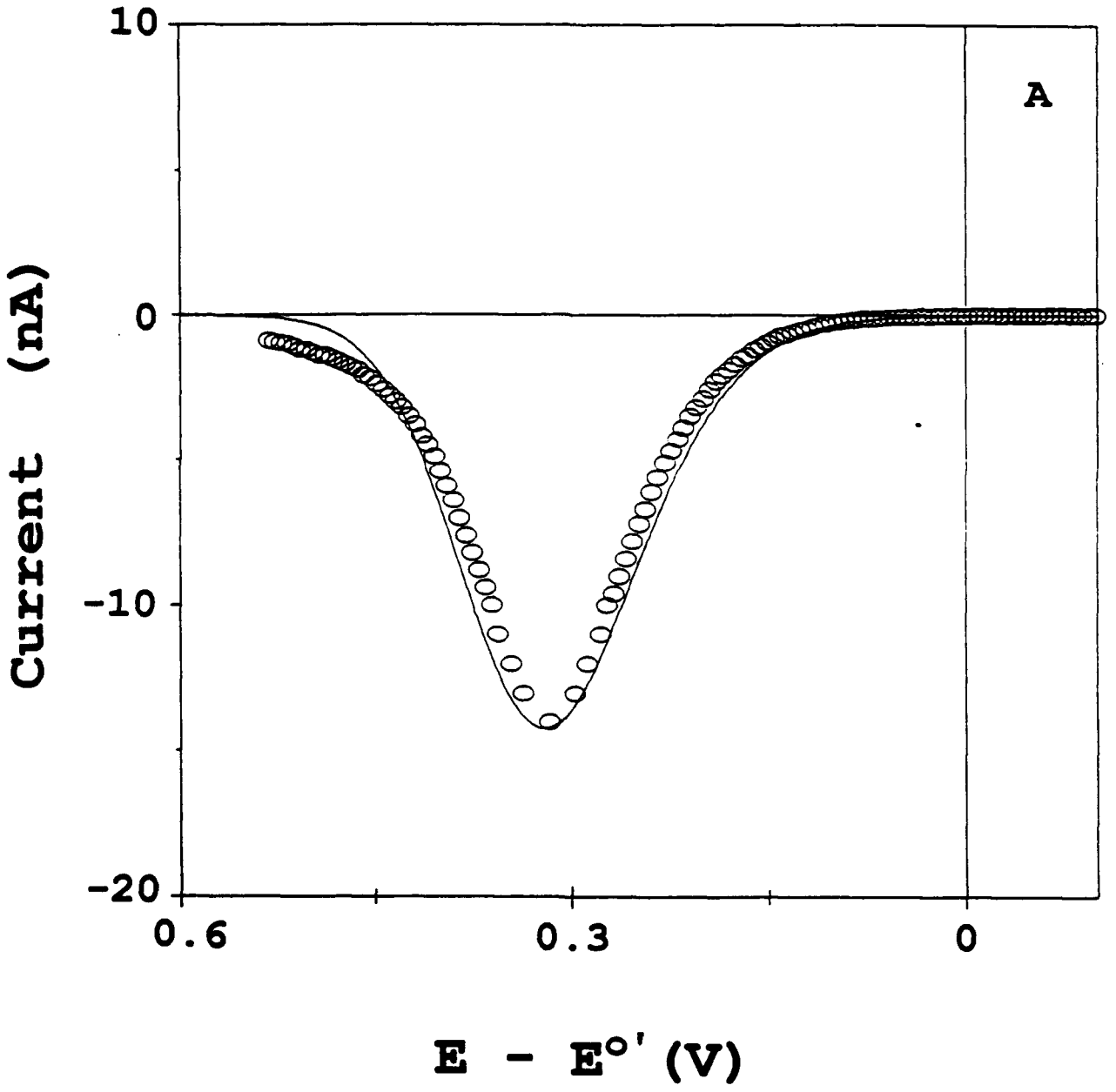

Fig 11

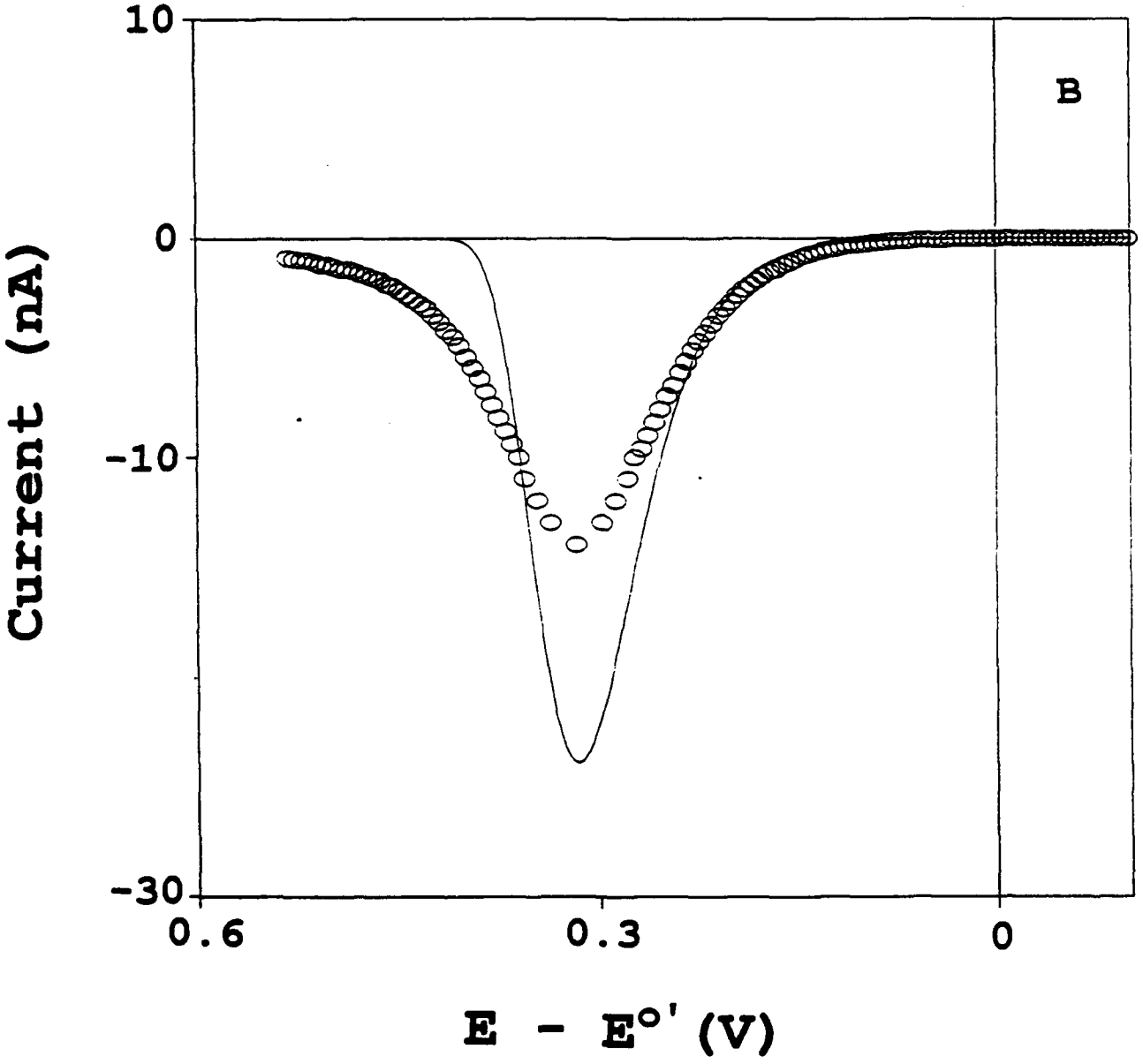
10
0
-10
-30
0.6
0.3
0
B
Current (nA)
E - E°' (V)